

# On the Modeling of Electrical Effects Experienced by Space Explorers During Extra Vehicular Activities: Intracorporal currents, Resistances, and Electric Fields.

Carlos J. Cela, *Member, IEEE*, Kyle Loizos, *Student Member, IEEE*, Douglas Hamilton, *Member, IEEE*, Raphael C. Lee, *Fellow, IEEE*, and Gianluca Lazzi, *Fellow, IEEE*

**Abstract**—Recent research has shown that space explorers engaged in Extra Vehicular Activities (EVAs) may be exposed, under certain conditions, to undesired electrical currents. This work focuses on determining whether these undesired induced electrical currents could be responsible for involuntary neuromuscular activity in the subjects, possibly caused by either large diameter peripheral nerve activation or reflex activity from cutaneous afferent stimulation. An efficient multiresolution variant of the admittance method along with a millimeter-resolution model of a male human body were used to calculate induced electric fields, resistance between contact electrodes used to simulate the potential exposure condition, and currents induced in the human body model. Results show that, under realistic exposure conditions using a 15V source, current density magnitudes and total current injected are well above previously reported startle reaction thresholds. This indicates that, under the considered conditions, the subjects could experience involuntary motor response.

## I. INTRODUCTION

UNDER certain circumstances, Extravehicular activity (EVA) adjacent to the International Space Station (ISS) can be associated with risk of electrical shock to the astronaut. During EVA the astronaut wears a specialized suit with a cooling undergarment connected to a heat exchanger apparatus. Despite the cooling mechanism, the astronaut often becomes soaked in perspiration while working on the exterior of the ISS. The sweat soaked undergarment is in direct contact with metal coupling rings in the Extravehicular Mobility Unit (EMU, Figure 1) and the astronaut's body.

When the astronaut exits the ISS, a steel safety cable is attached from the EMU's waist ring to the ISS. This electrically clamps the waist ring potential to that of the ISS. The ISS is immersed in Earth's ionosphere. Therefore, when the astronaut exits the ISS door, he enters conducting plasma. The rotation of the Earth's magnetic field through the conducting plasma induces currents, along with the corresponding electrical potential gradients. As the astronaut moves away from the ISS door, the voltage of the EMU relative to the ISS changes. The circuit that enables unwanted electrical shock is

Carlos J. Cela, Kyle Loizos, and Gianluca Lazzi are with the Department of Electrical and Computer Engineering, University of Utah, Salt Lake City, UT, USA. Douglas Hamilton is with NASA, Johnson Space Center, TX, USA. Raphael C. Lee is with the Medical Center of the University of Chicago, Chicago, IL, USA.



Fig. 1. Extravehicular Mobility Unit (EMU). Green bands correspond to places where metal is in contact with both the astronaut's skin and ionosphere's plasma.

formed by the ISS, the steel cable connecting the waist ring of the EMU, the astronaut, other rings in different locations in the EMU (Figure 1), and the plasma of the ionosphere.

To estimate the risk of involuntary muscular activation, the electric field strength induced in the body, the dynamics of the change in field strength, and the threshold fields and currents for nerve or muscle activation need to be considered. Because large sensory and motor neurons are much more sensitive to electric field stimulation than with direct stimulation of skeletal muscle, considering only nerve excitation is adequate for determining maximum risk. The purpose of this study is to determine the possibility of electrical shock induced involuntary neuromuscular activity resulting from EVA.

We investigated two different current paths through the body. The objective was to predict anatomical regions in which neurons of different diameters would be excited by electrical shocks consistent with those anticipated during EVA.

A first numerical model, which calculated the distribution of electric fields (E-fields) in the body, was built and solved using a multi-resolution variant of the admittance method [1][2]. The current paths were determined by the location

of electrical contact with metal coupling rings in the EMU, each having  $100\text{ cm}^2$  area. The first current path was from the sweat-soaked left anterior chest to the right waist. A second path was from the left wrist to the right waist. The electrical stimulus considered in the simulation was a  $4\text{ms}$ ,  $15\text{V}$ , electrical pulse, assuming sub-millisecond rise time. For the purposes of defining tissue conductivity, an operational frequency of  $10\text{kHz}$  was assumed. The tissue conductivities considered are listed on Table I. To address the probability of involuntary nerve excitation, the electric field distribution within major peripheral nerves was determined, as well as current densities and total current injected in the vicinity of the metal contacts. The possibility of reflex activity from cutaneous afferent stimulation is weighted in the context of known experimental studies [3], and on a second phase of this work, the occurrence of nerve excitation on terminal endings of peripheral nerve will be estimated with the help of the Spatially Extended Nonlinear Node (SENN) model [4][5].

The calculated body impedance was consistent with measured values under condition of wet skin. The peak current injected by a  $15\text{V}$  contact was  $18\text{mA}$  for the chest-to-hip current path and  $15\text{mA}$  for the wrist-to-hip current path; both of these values are well within the order of the current threshold for startle response [3]. Based on these results, a conclusion of no electrical hazard is not supportable.

## II. METHOD

A discrete model was derived from the Visible Human Male dataset [6]. The resolution of the model was  $1\text{ mm}$  and its size  $586 \times 340 \times 1878$  voxels. Tissue conductivities were taken at  $10\text{ kHz}$  from [7] and reported in Table I.

A software program was written to insert two circular cutaneous electrode pads in the numerical model. At  $1\text{ mm}$  resolution, a radius of 56 voxels was used for each electrode pad to approximate a total contact surface of  $100\text{ cm}^2$ . The current return electrode was positioned on the right side of the lumbar region. Two different stimulating electrode placement cases were studied, the first one on the chest, and the second on the wrist as shown on Figure 2. The skin was removed from the model under the electrodes to obtain perfect contact, but the skin impedance was included as a  $300\Omega$  per contact series resistance later in the numerical simulation. This series resistance value fits within the range considered by [7] and [8] for similar conditions.

A DC current injection of  $1\text{A}$  was considered for the stimulation, with its source at the chest (or wrist) electrode, and its sink at the hip electrode. The hip electrode was considered the electrical ground as well.

The admittance method was used to numerically solve the resulting electrical state. Because of the large model size, in excess of 335 million voxels, a multiresolution meshing algorithm [1][2] was used to reduce the order of the model by joining adjacent voxels inside large homogeneous portions of the body, while preserving higher level of detail at material boundaries. Each voxel was then represented as a network of lumped electrical elements [1] and all partial networks were joined into a large electrical network representing the entire

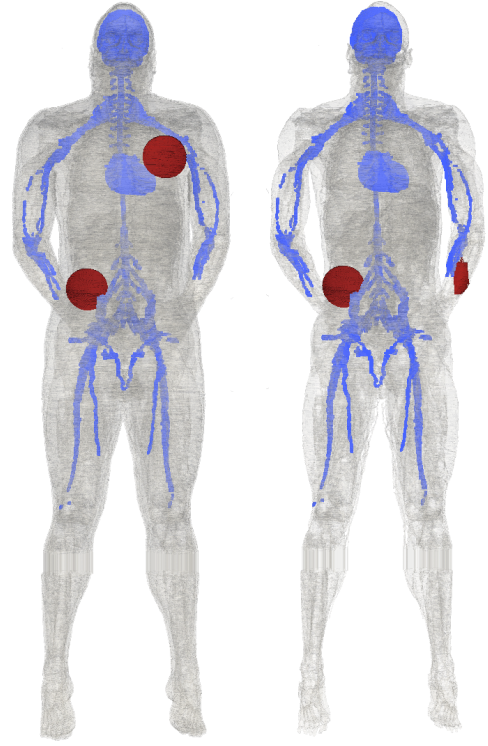


Fig. 2. Numerical model, based on the Visible Human Male 1mm dataset (frontal view). Nerves, heart and brain are shown in blue color for anatomical reference. Electrodes are represented in red color. Two cases were considered for electrode placement: chest to hip path (left) and wrist to hip path (right).

model. A linear system was then formed and solved using a preconditioned biconjugate gradient method; the result of this operation was the electrical potential at every point in the model.

Since  $1\text{A}$  was the injected current, the resulting calculated potential between the electrodes corresponds to the impedance between electrode pads. All the voltages were normalized so that the voltage between stimulating electrode pads was  $15\text{V}$ ; the E field magnitude was then calculated from the scalar electric potential field and voxel dimensions. A software program was written and used to filter out all the E field magnitude values outside the nervous system and heart, and to convert the simulation result to a format compatible with ParaView [9] for visualization.

## III. RESULTS

### A. Body Resistance and Total Current Injected

The simulations were run with a  $1\text{A}$  DC current from electrode to electrode to obtain body resistance, and subsequently scaled to the equivalent of  $15\text{V}$  between electrodes. In our model, the skin under the electrodes was removed to obtain perfect contact with the underneath tissue, but later added as a  $300\Omega$  series bulk resistance per electrode. A second simulation to verify the results obtained with the skin as described above was also performed. For this later case the model was reconstructed and a layer of skin under the electrodes was introduced; results obtained with the added skin

TABLE I  
TISSUE CONDUCTIVITIES AT 10 kHz [7]

Tissue	$\sigma$ [ $\Omega \cdot m$ ]
Bladder	2.130E-01
Blood	7.000E-01
Blood Vessel	3.131E-01
Body Fluid	1.500E+00
Bone Cancellous	8.262E-02
Bone Cortical	2.043E-02
Bone Marrow	2.735E-03
Brain Grey Matter	1.149E-01
Brain White Matter	6.948E-02
Cartilage	1.759E-01
Cerebellum	1.349E-01
Cerebro Spinal Fluid	2.000E+00
Colon	2.399E-01
Cornea	4.425E-01
Eye Sclera	5.103E-01
Fat	2.383E-02
Gall Bladder	9.001E-01
Gall Bladder Bile	1.400E+00
Gland	5.297E-01
Heart	1.542E-01
Kidney	1.377E-01
Lens	3.354E-01
Liver	5.350E-02
Lung Deflated	2.429E-01
Lung Inflated	9.317E-02
Lymph	5.297E-01
Metal	1.000E+04
Mucous Membrane	2.932E-03
Muscle	3.408E-01
Nail	2.043E-02
Nerve	4.240E-02
Pancreas	5.297E-01
Retina	5.103E-01
Skin Dry (body)	2.041E-04
Small Intestine	5.597E-01
Spleen	1.108E-01
Stomach	5.297E-01
Tendon	3.864E-01
Testis	4.298E-01
Tooth	2.043E-02
Vitreous Humor	1.500E+00

layer were in good agreement with those considering the skin as a series resistance.

In the chest-to-hip configuration, the largest resulting voltage in the model for 1A injection was 202V. From this, the resistance between electrodes without considering contact capacitances or skin is 202 $\Omega$ . Scaling for 15V requires a scaling factor of 15V/202V = 0.074; this results in a total injected current between electrodes of 74mA when 15V are applied, without considering the effect of the skin or contact capacitances. Considering the effect of the skin as a bulk resistance of 300 $\Omega$  per electrode contact in series, the total resistance for the chest-to-hip configuration is 300 $\Omega$ +202 $\Omega$ +300 $\Omega$  = 802 $\Omega$ . Thus, the total current injected for a 15V pulse in the chest-to-hip configuration and considering the effect of the skin is 74mA  $\times$  202 $\Omega$ /802 $\Omega$  = 18mA.

Similarly, for the wrist-to-hip configuration a resistance between electrodes of 369 $\Omega$  was calculated without considering the effect of the skin and contact capacitances, yielding a total injected current of 40mA for 15V. When the effect of skin under electrodes was taken into account, a resistance of 969 $\Omega$  was estimated and a current of 15mA.

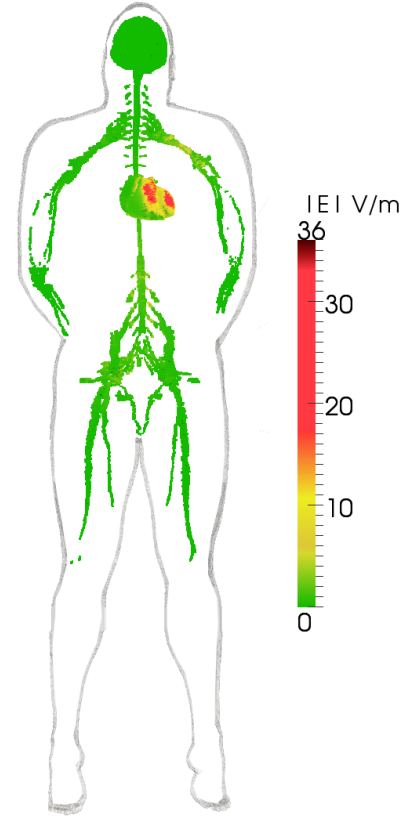


Fig. 3. Electric field in excitable tissue caused by a 15V electric shock for chest-to-hip configuration.

#### B. Electric Fields and Induced Current Densities Near the Electrodes

The electric field magnitudes were calculated from the electric potentials and mesh geometry. We were interested in the electric field present in excitable tissue, namely peripheral nerves, heart, and brain. Figure 4 and Figure 4 show the electric fields on excitable tissue for both configurations modeled.

The current density magnitudes at each point in the model were calculated from the electric fields and dielectric properties of the tissues. We were particularly interested in quantifying current densities close to the electrodes, where they are presumed to be larger, and in proximity of cutaneous afferent neurons. The current density magnitudes at a transverse plane crossing the center of each stimulating electrode are plotted in Figure 5 and Figure 6 for the chest-to-hip case and on Figure 7 for the wrist-to-hip case.

#### IV. DISCUSSION

We presented a study to help determine the possible effects of undesired induced electric currents and the possibility of inducing involuntary neuromuscular activity when the space explorer is outside the ISS. Because of the relatively coarse resolution of our model compared with finer nerve structures, only large peripheral nerves are represented. We considered the possibility of accidental activation of larger diameter peripheral nerves, cardiac fibrillation, and cutaneous afferent neuron activation. For the purpose of this discussion, we will focus on the latter effect.

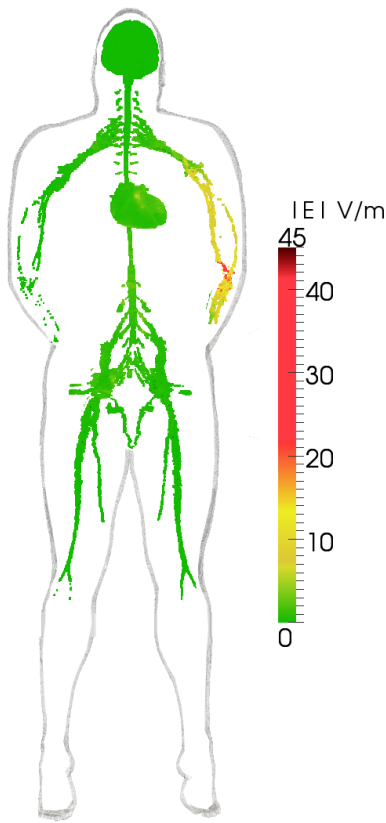


Fig. 4. Electric field in excitable tissue caused by a 15V electric shock for wrist-to-hip configuration.

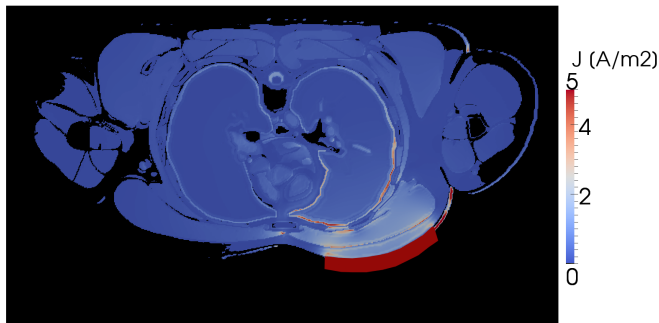


Fig. 5. Chest-to-hip configuration. Transverse slice through center of electrodes, frontal aspect of body towards bottom of plot. Current density magnitudes in the proximity of chest electrode for 15V shock.

Direct effect of stimulation of sensory nerves in the skin was not computable, since single axons are not resolvable with the mesh resolution of the considered model. However, values for current density magnitudes and total current injected were calculated for areas close to the stimulating electrodes, and can be used to compare to previously reported experimental data. Current values injected for a 15 V shock are in the range of 15mA to 18mA, and well above the startle reaction current thresholds reported by [3]. Thus, we conclude that the risk of involuntary motor response is likely with a 15V electric shock, under the assumptions of the model.

We should also note that cutaneous nerves are primary sensory, and stimulation of these nerves due to the electric shocks is likely to produce spinal withdrawal reflexes, which

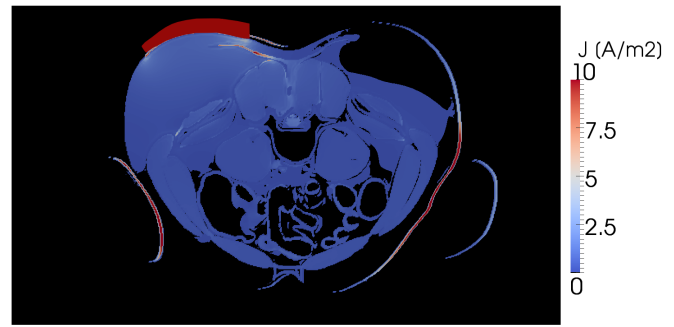


Fig. 6. Chest-to-hip configuration. Transverse slice through center of electrodes, frontal aspect of body towards bottom of plot. Current density magnitudes in the proximity of hip electrode for 15V shock.

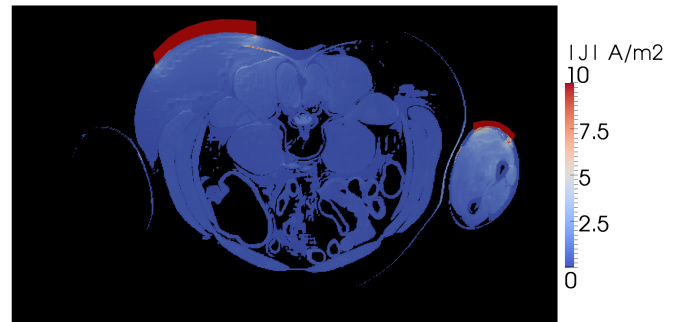


Fig. 7. Wrist-to-hip configuration. Transverse slice through center of hip electrode, frontal aspect of body towards bottom of plot. Current density magnitudes in the proximity of hip (left) and wrist (right) electrodes for 15V shock

may cause for a generalized involuntary motor response in the entire body.

## REFERENCES

- [1] C. J. Cela. *A Multiresolution Admittance Method for Large-Scale Bioelectromagnetic Interactions*. PhD thesis, North Carolina State University, 2010.
- [2] C. J. Cela, Raphael C. Lee, and G. Lazzi. Modeling cellular lysis in skeletal muscle due to electric shock. *IEEE Trans. Biomed. Eng.*, PP(99), 2011.
- [3] IEC/TR. Effects of current on human beings and livestock - part 5: Touch voltage threshold values for physiological effects. TR 60479-5, International Electrotechnical Commission, Geneva, Switzerland, 2007.
- [4] J. Patrick Reilly, Vanda T. Freeman, and Willard D. Larkin. Sensory effects of transient electrical stimulation - evaluation with a neuroelectric model. *IEEE Trans. Biomed. Eng.*, BME-32(12), 1985.
- [5] J. Patrick Reilly and Alan M. Diamant. Spatial relationships in electrosimulation: Application to electromagnetic field standards. *IEEE Trans. Biomed. Eng.*, 50(6), 2003.
- [6] V. Spitzer, M. J. Ackerman, A. L. Scherzinger, and D. Whitlock. The visible human male: A technical report. *J. Am. Med. Inform. Assoc.*, 3(2), April 1996.
- [7] S. Gabriel, R. W. Lau, and C. Gabriel. The dielectric properties of biological tissues: Iii. parametric models for the dielectric spectrum of tissues. *Phys. Med. Biol.*, 41:2271–2293, 1996.
- [8] IEC/TR. Effects of current on human beings and livestock – part 1: General aspects. TR 60479-1, International Electrotechnical Commission, Geneva, Switzerland, 2007.
- [9] A. Henderson. *ParaView Guide, A Parallel Visualization Application*. Kitware Inc., 2007.